Corrosion behavior of biomedical AZ91 magnesium alloy in simulated body fluids

Yunchang Xin
Department of Physics and Materials Science, City University of Hong Kong, Kowloon, Hong Kong, People's Republic of China; and Advanced Materials Institute, Tsinghua University, Shenzhen Graduate School, Shenzhen 518055, People's Republic of China

Chenglong Liu
Department of Physics and Materials Science, City University of Hong Kong, Kowloon, Hong Kong, People's Republic of China

Xinmeng Zhang
State Key Laboratory of Welding Production Technology, School of Materials Science and Engineering, Harbin Institute of Technology, Harbin 150001, China

Guoyi Tang[a)]
Advanced Materials Institute, Tsinghua University, Shenzhen Graduate School, Shenzhen 518055, People's Republic of China

Xiubo Tian
State Key Laboratory of Welding Production Technology, School of Materials Science and Engineering, Harbin Institute of Technology, Harbin 150001, China

Paul K. Chu[b)]
Department of Physics and Materials Science, City University of Hong Kong, Kowloon, Hong Kong, People's Republic of China

(Received 13 February 2007; accepted 29 March 2007)

Fast degradation rates in the physiological environment constitute the main limitation for magnesium alloys used in biodegradable hard tissue implants. In this work, the corrosion behavior of AZ91 magnesium alloy in simulated body fluids (SBF) was systematically investigated to determine its performance in a physiological environment. The influence of the main constituent phases on the corrosion behavior was studied by in situ visual observation and scanning electron microscopy. Energy dispersive x-ray spectrometry and Fourier transfer infrared spectroscopy revealed that both calcium and magnesium phosphates are present in the corroded products besides magnesium oxide. Electrochemical methods including open circuit potential evolution and electrochemical impedance spectroscopy were used to investigate the mechanism. The corresponding electrode controlled processes and evolution of the corrosion products layer were discussed. The degradation rate after immersion in SBF for seven days was calculated from both the weight loss and hydrogen evolution methods.

I. INTRODUCTION

Because of their high strength, ductility, and good corrosion resistance, metallic materials such as stainless steels, cobalt-based alloys, and titanium alloys constitute an important class of materials for hard tissue replacements, especially load-bearing implants. However, because these materials do not degrade spontaneously after implantation into the human body, a second surgical procedure may be necessary after the tissues have healed. Repeated surgeries increase the costs as well as patient morbidity. In addition, mismatch of the elastic moduli between metallic biomaterials and natural bone results in stress shielding effects that can lead to reduced new bone growth.[1] In this respect, biodegradable magnesium-based alloys have potential applications, and good biocompatibility has in fact been observed in clinical and in vivo and in vitro assessments.[2–4] Unfortunately, pure magnesium and its alloys corrode too quickly at the physiological pH (7.4–7.2) as well as in physiological media containing high concentrations of chloride ions, thereby losing mechanical integrity before the tissues have sufficient time to heal. Furthermore, during the corrosion

Address all correspondence to these authors.
[a)]e-mail: tanggy@mail.sz.tsinghua.edu.cn
[b)]e-mail: paul.chu@cityu.edu.hk
DOI: 10.1557/JMR.2007.0233

 © 2007 Materials Research Society

process, release of hydrogen gas may be too fast to be endured by the host tissues.[1]

The corrosion behavior of magnesium alloys in chloride solutions has been studied.[5–8] The electrode controlled processes such as mass transfer, charge transfer, and evolution of corrosion byproducts have been investigated by electrochemical techniques such as electrochemical impedance spectroscopy (EIS) and open circuit potential evolution.[6,8–11] It is known that the environment has a large influence on the corrosion behavior. For instance, the physiological environment contains many other ions including phosphates, sulfates, and carbonates in addition to chlorides that can attack the materials,[12] and the alloys may corrode differently. Studies by Kuwahara and Witte have contributed to the understanding of the behavior of biomedical magnesium alloys in Hank's solution as well as in vivo and in vitro environments.[1,13–17] However, most of these studies focus on degradation behavior in the physiological environment or interaction with body tissues and do not address in detail the electrochemical behavior. Therefore, they do not provide detailed information about electrode-controlled processes in the alloy/solution system and their variation with immersion time. EIS is a powerful technique for studying the electrochemical corrosion processes on metals and coated metals. When a small amplitude excitation signal is applied to the system, its response depends on the electrode kinetics processes. It usually consists of several different subprocesses including mass transfer, charge transfer, and so on. By analyzing these responses, the individual processes may be deduced.[8,18] Combining results of EIS and other electrochemical tests such as potentiodynamic polarization and open circuit potential evolution leads to a better understanding of the corrosion process of alloys.

In this work, the electrochemical behavior of AZ91 magnesium alloys in simulated body fluids (SBF) was systematically investigated by open-circuit potential evolution and EIS. The corrosion mechanism and electrode controlled processes are discussed. The degradation rate in SBF is gauged by both hydrogen evolution and weight loss.

II. EXPERIMENTAL DETAILS

A. Sample preparation

Commercially available extruded AZ91 Mg alloys provided by YiHo Corporation, Shenzhen, China were used. Their compositions are listed in Table I. The dimensions of the samples used in the experiments were 15 mm × 15 mm × 3 mm. They were ground with #4000 waterproof diamond paper followed by ultrasonic cleaning in alcohol.

TABLE I. Composition of AZ91 magnesium alloys.

	Al	Zn	Mn	Si	Fe	Ni	Cu
AZ91	8.5–9.5	0.45–0.9	0.17–0.5	<0.05	<0.004	<0.001	<0.015

B. In situ visual observation and corrosion product identification

After the samples were taken out of the test solution and exposed to air, the surface turned white, and the morphology changed as well.[5] Therefore, the corrosion morphology was observed in situ by optical microscopy. The micromorphologies after immersion in SBF for 1 day, 4 days, and 7 days were also observed by scanning electron microscopy (SEM). The composition of the corrosion products was determined by energy dispersive x-ray spectroscopy (EDS). Fourier transform infrared (FTIR) spectroscopy was conducted from 4000 to 400 cm^{-1} to identify the functional groups in the corrosion products.

C. Electrochemical behavior

The electrochemical corrosion behavior was investigated by open-circuit potential evolution (E_{corr}-t) and EIS using Gamry Reference 600 (Gamry Instruments, Warminster, PA). The ion concentrations in the SBF are shown in Table II.[19] A three-electrode cell with the sample as the working electrode, saturated potassium chloride electrode as the reference electrode, and platinum electrode as the counter electrode was used. In the E_{corr}-t test, changes in the open circuit potential were monitored as a function of immersion time for about 240 ks. The data were recorded every 120 s. The impedance data were recorded from 100 kHz to 10 mHz with a 10 mV sinusoidal perturbing signal. The lowest frequency was set to 10 mHz to reduce the time and potential noise interference. The EIS measurement may be affected by phase shifts from the potentiostat in the high frequency region, so the upper frequency limit was set at 100 kHz.[18] In the EIS measurement, the sample was immersed in the test solution until the final test had been completed. All the electrochemical tests were carried out at room temperature.

D. Degradation rate measurement

The hydrogen evolution rates and corresponding degradation rates were monitored as a function of immersion time. The average degradation rates after immersion in

TABLE II. Ion concentrations in simulated body fluids (SBF).

Concentration (mmol/l)	Na^+	K^+	Ca^{2+}	Mg^{2+}	HCO_3^-	Cl^-	HPO_4^{2-}	SO_4^{2-}
SBF	142.0	5.0	2.5	1.5	4.2	148.5	1.0	0.5
Blood plasma	142.0	5.0	2.5	1.5	27.0	103.0	1.0	0.5

SBF at about 37 °C for 7 days were calculated by means of weight loss and hydrogen evolution. In the hydrogen evolution method depicted in Fig. 1, the hydrogen evolution volume was measured, and the degradation rate was deduced from the reaction below:

$$Mg + 2H_2O \rightarrow Mg(OH)_2 + H_2 \uparrow \quad . \qquad (1)$$

In the weight loss method, the corroded specimens were removed from the test solution after immersion, cleaned with distilled water, and dried. They were subsequently immersed in chromate acid (200 g/l CrO_3 + 10 g/l $AgNO_3$) for 5–10 min to remove the corrosion products. Afterwards, the specimens were washed with distilled water and dried again. The dried specimen was weighed, and the degradation rate was calculated as follows:

$$DR = \frac{W}{At} \quad , \qquad (2)$$

where *DR* refers to the degradation rate, *W* is the weight loss from the sample, and *A* and *t* represent the exposure area and exposure time in SBF, respectively.

III. RESULTS AND DISCUSSION

A. In situ visual observation and corrosion products

It is well known that secondary phases have a pronounced influence on the corrosion resistance of magnesium alloys. The AZ91 magnesium alloy is a typical two-phase material. The high Al content often exists in the form of the β phase ($Mg_{17}Al_{12}$) along the grain boundaries.[6] As shown in Fig. 2, the β phase (denoted by arrows) can be seen after polishing. The β phase has two main forms, the fine β phase and continuous β phase. When the materials are soaked in SBF, corrosion takes place on the entire surface with evolution of hydrogen. Hydrogen bubbles are retained on the surface by surface tension. Based on the photograph taken after 2 min, intense corrosion (denoted by arrows) preferentially initiates form the boundary where the β phase contacts the surrounding matrix, the α phase. The photographs taken after 2 h reveal serve corrosion around the fine β phase. However, a different situation is observed from the continuous β phase. Here, spreading of corrosion along the matrix tends to be blocked. After 2 h of immersion, the matrix around the fine β phase has completely corroded whereas no corrosion is observed from the adjacent β phase. $Mg_{17}Al_{12}$ exhibits a more passive behavior over a wide pH range than either Al or Mg and is found to be inert in chloride solutions in comparison with the Mg matrix. It thus can serve as a corrosion barrier.[12] Its barrier role is, however, limited to precluding corrosion from spreading laterally or progressing deeply into the matrix. On the other hand, the β phase is cathodic with respect to the matrix.[6] It can significantly accelerate the matrix corrosion rate by forming micro-galvanic couples between the β phase and matrix. It should also be mentioned that filiform corrosion is not observed during the entire immersion duration.

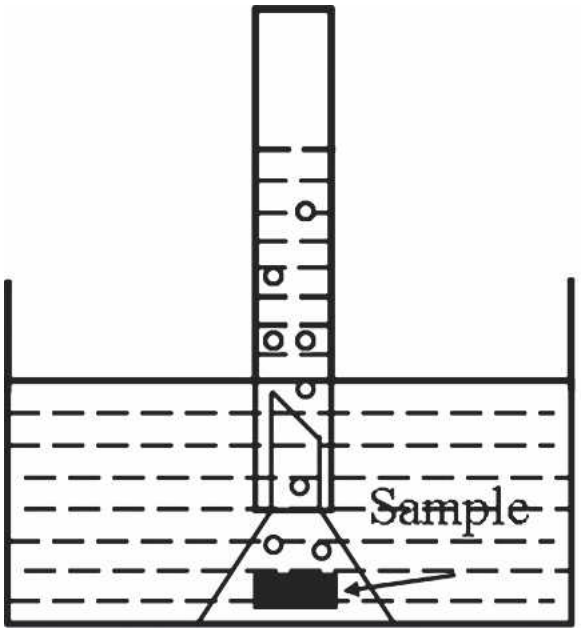

FIG. 1. Schematic illustration of the hydrogen evolution volume measurement.

The microcorrosion morphologies after immersion in SBF for 1, 4, and 7 days are monitored by SEM. The composition of the corrosion products is determined by EDS, and the results are shown in Fig. 3. All the surfaces after immersion for the three different durations are found to have corroded completely as manifested by cross-linked cracks. The presence of cracks may be attributed to dehydration of the corroded layer after drying in warm air and in the SEM vacuum chamber. The EDS spectra disclose that the corrosion products are mainly composed of Mg, Al, Zn, P, Ca, and O. The Ca to P atomic ratios are about 0.44, 0.60, and 0.55 after immersion for 1, 4, and 7 days, respectively, and they are much lower than those of calcium phosphates.[20] The weight percent of magnesium in the corrosion products after immersion for 4 and 7 days are much lower than that after immersion for 1 day, but those of P, O, and Ca are higher, implying accumulation of corrosion products and richer phosphates in the corrosion products. The elemental weight percents in the corrosion products are similar after immersion for 4 and 7 days.

The FTIR spectra acquired from the samples soaked in SBF for 1, 4, and 7 days are displayed in Fig. 4. The three spectra are quite similar. A broad OH^- absorption band

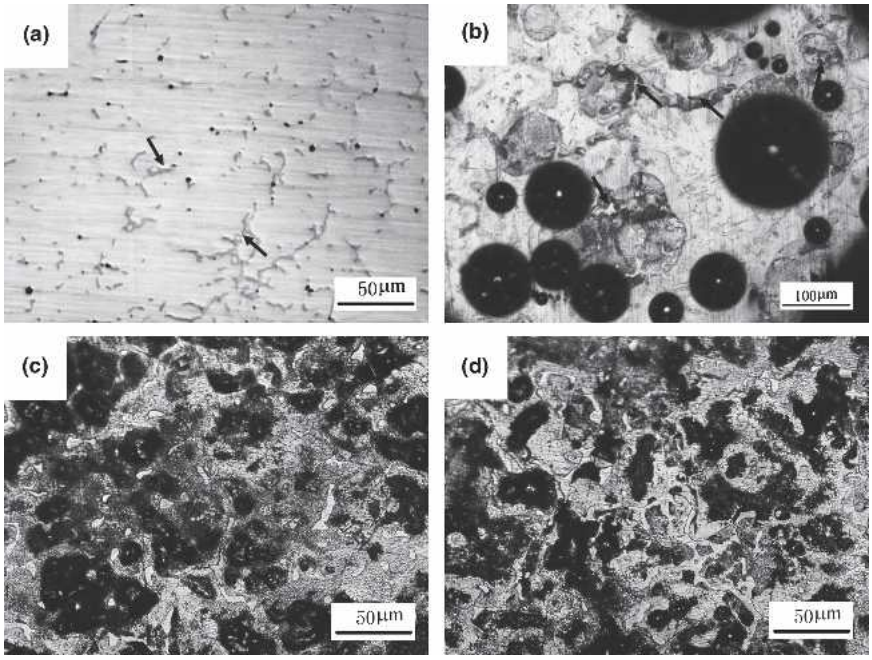

FIG. 2. In situ observation of the corroded micromorphology of samples soaked in SBF: (a) before immersion, (b) after immersion for 2 min, (c) after immersion for 2 h, and (d) after immersion for 2 h.

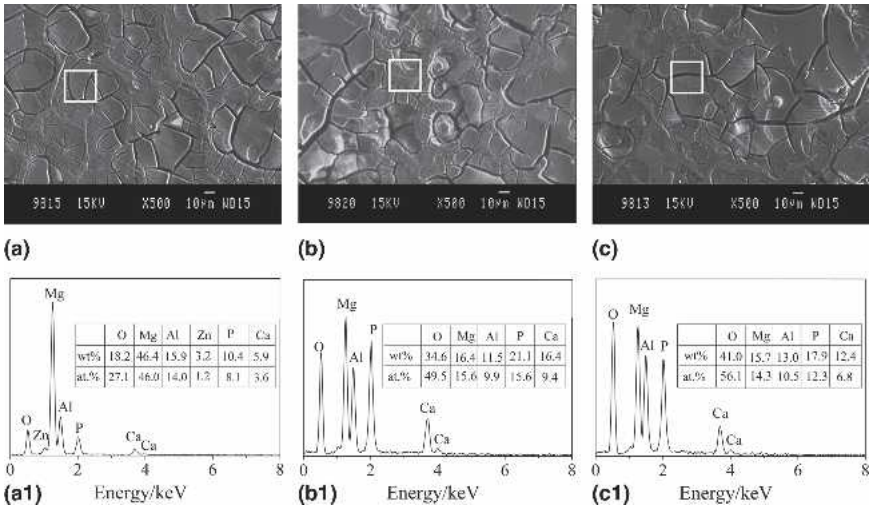

FIG. 3. SEM corrosion morphology of samples after soaking in SBF for different periods of time and EDS spectra obtained from selected regions denoted by rectangle: A – 1 day immersion, A1 – EDS spectrum of A; B – 4 days immersion, B1 – EDS spectrum of B; C – 7 days immersion, and C1 – EDS spectrum of C.

from 3700 to 2500 cm^{-1} and a weak water absorption band at around 1650 cm^{-1} are observed. The obvious absorption bands at 1160 and 1040 cm^{-1} correspond to phosphates, and the weak, broad band from 1400 to 1550 cm^{-1} originates from carbonates.[21] According to Canham and co-workers,[22] a sharp P–O bending mode doublet at 600 cm^{-1} is indicative of the crystalline phase of hydroxyapatite. No such absorption mode is observed from these three samples. The absorption peak at 520 cm^{-1} is from Mg–O (MgO).[23]

When the sample is exposed to an aqueous corrosion medium, the following reactions take place[12]:

$$\begin{aligned} Mg &\rightarrow Mg^{2+} + 2e^{-} \quad , \\ 2H_2O + 2e^{-} &\rightarrow H_2 + 2(OH)^{-} \quad , \\ Mg^{2+} + 2(OH)^{-} &\rightarrow Mg(OH)_2 \quad . \end{aligned} \tag{3}$$

When the sample is taken out of the solution, $Mg(OH)_2$ transforms to hydrated magnesium oxide ($MgO{\cdot}H_2O$),[8] as corroborated by FTIR. It is believed that the absorbed Mg ions block the surface growth sites of the calcium phosphate crystals and thus suppress homogeneous crystallization of calcium phosphate in the Mg^{2+} containing solution.[20] The solubility of most calcium phosphates

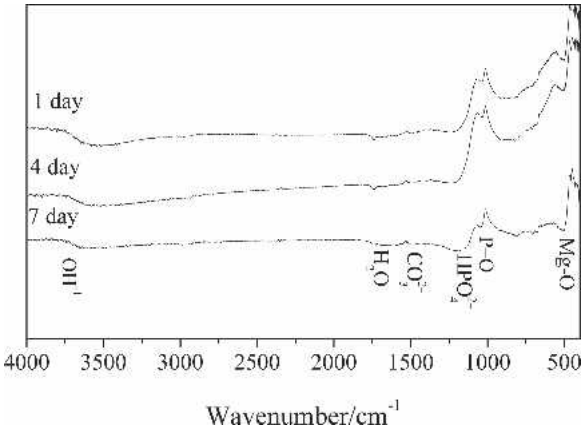

FIG. 4. FTIR spectra of AZ91 magnesium alloy after soaking for different durations.

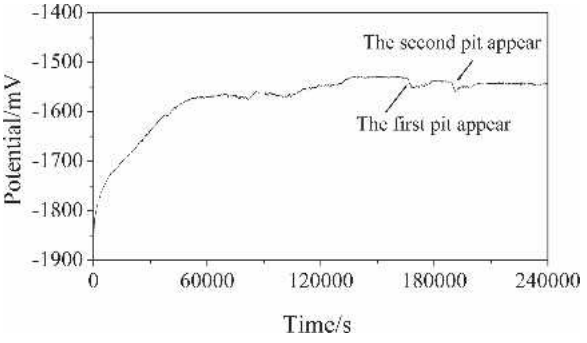

FIG. 5. Open-circuit potential of AZ91 magnesium alloy as a function of immersion time.

such as hydroxyapatite and tricalcium phosphate decreases at higher pH values.[24] During corrosion, a large amount of Mg ions dissolve into the test solution and the pH value increases due to reaction (3). The high Mg ion concentration depresses precipitation of calcium phosphate. Hence, the increase in the pH value is believed to play a crucial role in the precipitation of calcium phosphate. In the SBF, insoluble tertiary magnesium phosphate, $Mg_3(PO_4)_2$, may also precipitate as the corrosion products from the following reaction[25]:

$$Mg(H_2PO_4)_2 + 4H_2O \rightarrow Mg_3(PO_4)_2 \cdot 4H_2O + 4H_3PO_4 \quad . \tag{4}$$

As discussed above, the pH value of the SBF increases because of reaction (3). Consumption of OH^- by H_3PO_4 accelerates the forward reaction (4) and stimulates precipitation of insoluble $Mg_3(PO_4)_2$. Precipitation of magnesium phosphates thus appears to be the reason for the low Ca to P ratio in the corrosion products. Li et al.[26] have demonstrated that the pH value of SBF in contact with pure magnesium increases quickly initially and becomes constant after about 3 days. The stable pH value implies a balance between the formation and dissolution of the corrosion products and may be the reason for the similar elemental weight percents in the corrosion products after immersion for 4 and 7 days.

B. Electrochemical behavior

The corrosion potential (E_{corr}) indicates that electrochemical reactions take place at the electrode–solution interface. The variations in the corrosion potential with immersion time can be used to study the reactions occurring at the electrode–solution interface. The typical E_{corr}-t curve acquired from the AZ91 magnesium alloy is shown in Fig. 5. At the beginning, E_{corr} shifts to the positive direction gradually, and from about 50 ks, the potential stabilizes and large fluctuations cannot be observed during subsequent immersion. It is noted that at about 16.6 ks, a sudden drop in the corrosion potential appears, implying the occurrence of pitting corrosion. The same drop appears again at about 19 ks, indicating the formation of the second pit. A gradual increase in the corrosion potential follows the drop of the potential, indicating the self-limiting effect of pitting corrosion. This self-limiting effect is associated with the cathodic reaction.[12] A byproduct produced in the cathodic reaction is OH^-, which can raise the localized pH value, accelerating the formation and stabilization of the corrosion products, and hence pitting corrosion can be depressed gradually to some extent. When the magnesium alloy is exposed to the corrosion medium, chemical dissolution together with electrolyte penetration results in spontaneous corrosion on the entire surface, resulting in the formation of corrosion products, including magnesium hydroxide and magnesium phosphate, as discussed above. However, it is difficult for the corrosion products to precipitate in the microcathode (β phase) area where hydrogen is evolved. Due to diffusion of OH^-, the corrosion products precipitate mainly at the vicinity of the microanode (α phase).[18] As a result, the active region decreases, and protection by the corrosion products layer is enhanced progressively with longer exposure time. This is the reason why the corrosion potential shifts to the nobler direction. The origin of pitting corrosion in the magnesium alloy lies in the inhomogeneous crystal. In the AZ91 magnesium alloy, $Mg_{17}Al_{12}$ has a higher standard voltage[7] and forms an electrolysis junction with the surrounding matrix. Pits are often formed due to selective attack along the $Mg_{12}Al_{17}$ networks.[7] The corrosion product can depress this galvanic effect between the two phases.[18] After immersion for a sufficiently long time, the galvanic effect is depressed to some extent, and the corrosion mechanism changes from general corrosion to pitting corrosion. The critical chloride concentration required for pitting corrosion to occur on magnesium is about 30 mmol/L,[27] which is much lower than that in SBF that contains 142 mmol/l.[19] Hence, pitting corrosion is a common behavior of magnesium alloys exposed to SBF.

EIS is a powerful technique for studying the electrochemical corrosion process on metals. When an excitation signal with a small amplitude is applied to the system, the response depends on the electrode kinetics. It usually consists of several different subprocesses, including mass transfer, charge transfer, and so on. By analyzing these responses, the individual processes may be deduced.[18,28] The representative EIS spectrum acquired from the AZ91 magnesium alloy as a function of immersion time is displayed in Fig. 6. Comparing the impedance data obtained for different immersion duration, the EIS exhibits a pronounced and well-regulated evolution in both the high- and low-frequency regions with time. The high-frequency behavior of the EIS is associated with electrolyte penetration, including water uptake and electrolyte intrusion.[18] The properties of the corrosion products and alteration can be determined at high frequencies. Usually, the low-frequency region conveys important information about the electrode control process as well as the contribution from localized defects to the overall impedance.[18] Here, the variations at low frequencies may be attributed to changes in the corrosion product layer, and the evolution at low frequencies probably results from changes in the corrosion mode. After soaking in SBF, a corroded layer forms quickly, and two capacitive loops at high frequency and low frequency are observed in the Nyquist plot at the beginning of immersion. They generally result from charge transfer, effects of the corrosion products layer, and mass transfer.[18] Prolonging the immersion time leads to larger high- and low-frequency loops before 36 h. This variation in impedance is associated with thickening of the corroded layer and improved protection by this layer. From 36 h onward, only one capacitive loop appears with significantly reduced impedance, suggesting the presence of pitting corrosion. At 48 h, there is also only one capacitive loop with increasing impedance. This increase in the impedance also suggests the self-limiting effect of pitting corrosion. From the beginning of immersion, an inductive loop occurs at low frequencies and as time elapses, the inductive loop becomes more invisible before pitting corrosion. As mentioned above, the α matrix and β phase form galvanic couples, and intense corrosion occurs at the edge where the α matrix contacts the β phase. The presence of the inductive loop probably results from intense microgalvanic corrosion between the α matrix and β phase. With accumulation of the corrosion products, this galvanic-couple effect is depressed, and the inductive loop becomes more invisible as well. The EIS results are in good agreement with the open-circuit potential evolution test.

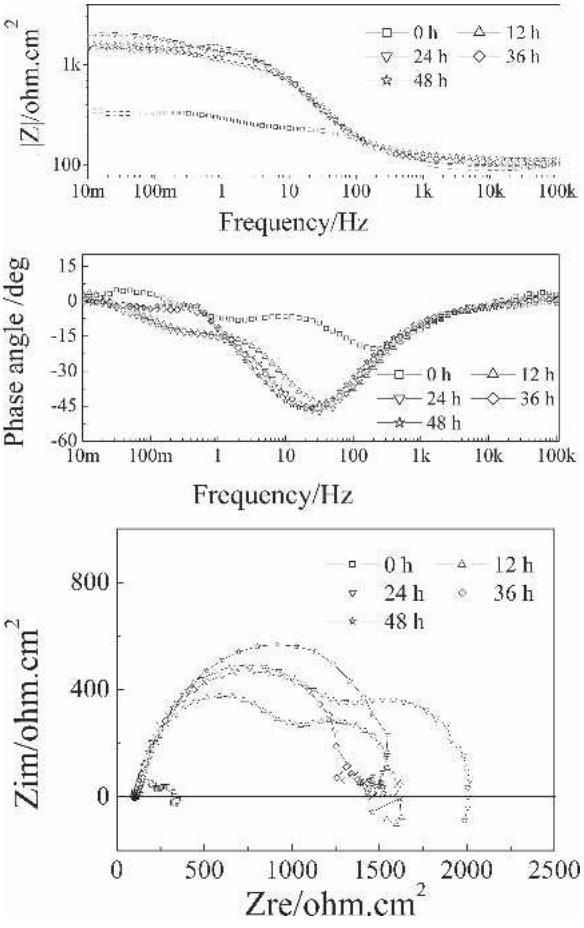

FIG. 6. Representative EIS of AZ91 magnesium alloy as a function of immersion time.

C. Degradation rate in SBF

As discussed in the previous section, reaction (1) takes place in an aqueous corrosion medium. The volume of evolved hydrogen is related to dissolution of magnesium. The corrosion products do not influence the relationship between hydrogen evolution and magnesium dissolution. The hydrogen evolution method is thus reliable, easy to implement, and not prone to errors inherent to weight loss measurements.[12] In addition, this technique has the advantage that variations in the degradation rates can be monitored by the hydrogen evolution rates, allowing the study of the degradation rate variation versus exposure time. It is known that hydrogen gas evolution during the corrosion process is too fast to be dealt with by the host tissues.[1] A study on the variation of the hydrogen evolution rate with exposure time is thus of great value. Considering the quick variation of the hydrogen evolution rates in the early stage, the measuring intervals are set small. Due to the small hydrogen volume at the latter stage, a larger interval is used. Figure 7 depicts the hydrogen evolution rates and corresponding degradation rates as a function of immersion time in SBF. The hydrogen evolution rate in the first 2 h is very high and drops significantly during the subsequent 4 h. It decreases more slowly after 6 h of immersion and stabilizes from about 44 h. The average degradation rates after

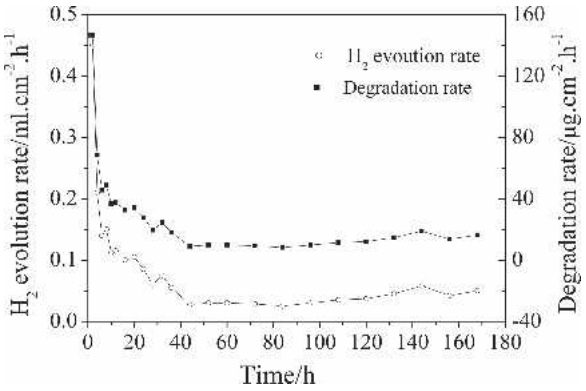

FIG. 7. Hydrogen evolution rates and corresponding degradation rates of AZ91 magnesium alloy as a function of immersion time.

immersion in SBF for 168 h calculated by the different methods are listed in Table III. The average degradation rate calculated by the hydrogen evolution method is about 0.43 mg.cm^{-2} day^{-1} and about 0.47 mg cm^{-2} day^{-1} by the weight loss method. The two results are quite consistent. The degradation rate calculated from the sample without removing the corrosion products is only about half that cleaned by chromate acid.

The high degradation rate of magnesium alloy in SBF stems from aggressive attack by chloride, sulfate, phosphate, and carbonate ions, among which chloride ions pose the biggest threat.[12] Chloride ions can transform the surface $Mg(OH)_2$ into more soluble $MgCl_2$. Dissolution of $Mg(OH)_2$ makes the surface more active or decreases the protected area, consequently promoting further dissolution of magnesium. Song et al. also suspect that chloride ions are involved in the intermediate step of magnesium dissolution by accelerating the electrochemical reaction rate from magnesium to magnesium univalent ions.[29] The reaction can be summarized as follows[27]:

$$\begin{aligned} Mg + H_2O &\rightarrow Mg(OH)_2 + H_2 \\ Mg + Cl^- &\rightarrow MgCl_2 \\ Mg(OH)_2 &\rightarrow MgCl_2 + Cl_2 \quad . \end{aligned} \tag{5}$$

As discussed above, precipitation of $Mg_3(PO_4)_2$ consumes OH^-, promotes the forward reaction, and stimulates dissolution of magnesium. The effects of carbonates tend to be more complex. They can accelerate or slow the corrosion rate of magnesium depending on the concentration of HCO_3^-. According to Geneviève's work,[8] when the concentration of HCO_3^- exceeds about 40 mg/L, the corrosion rate goes up due to accelerated dissolution of the $Mg(OH)_2$ (MgO) protection film. If the concentration is lower than this critical concentration, corrosion of magnesium can be retarded. The HCO_3^- concentration in the SBF is about 256 mg/L,[19] which is much higher than 40 mg/L. Hence, carbonates also increase the corrosion rate in SBF. Sulfates are also aggressive to magnesium but not to the extent of chloride ions.[29] On account of the large area of fresh surface and inferior protection offered by the corrosion products, intense corrosion takes place during early exposure, and the corrosion rate is high. Subsequent passivation of the active surface and accumulation of corrosion products decelerate corrosion. After immersion for a sufficiently long time, an equilibrium between the formation and dissolution of the corrosion products is established, leading to stable degradation rates.

TABLE III. Degradation rates of AZ91 magnesium alloy soaked in SBF for 168 h calculated from two different methods.

	Hydrogen evolution method	Weight loss method (with corrosion products)	Weight loss method (without corrosion products)
Degradation rates (cm^{-2}day)	0.43	0.23	0.47

IV. CONCLUSION

The corrosion behavior of AZ91 magnesium alloy immersed in SBF was studied by in situ visual observation, SEM, and electrochemical methods. The composition of the corrosion products was determined by EDS and FTIR. The average degradation rates and variations in the degradation rates with exposure time was determined from the immersion tests. The secondary phase (β phase) has a pronounced influence on corrosion. It accelerates the corrosion rates by forming galvanic couples, but the continuous β phase also tends to block the spreading of corrosion along the Mg matrix. Filiform corrosion is not observed during immersion in SBF. Besides magnesium oxide, both magnesium and calcium phosphate precipitate as the corrosion products. The phosphate contents increase with immersion time and stabilize after about four days of immersion. Pitting corrosion is a common behavior of AZ91 magnesium soaked in SBF, but is self-limited due to accumulation and stabilization of the corrosion products by OH^-. The corrosion rates that are very high during early exposure decrease significantly afterward and stabilize from about two days.

ACKNOWLEDGMENT

The project was supported by City University of Hong Kong Applied Research Grant (ARG) No. 9667002.

REFERENCES

1. M.P. Staiger, A.M. Pietak, J. Huadmai, and G. Dias: Magnesium and its alloys as orthopedic biomaterials: A review. *Biomaterials* **27,** 1728 (2006).
2. E.D. McBride: Absorbable metal in bone surgery. *JAMA* **111,** 2464 (1938).

3. J. Verbrugge: The metal material resorbable in osseous surgery. *Press Med.* **23,** 460 (1934).
4. J. Vormann: Magnesium: Nutrition and metabolism. *Mol. Aspects Med.* **24,** 27 (2003).
5. G.L. Song, A. Atrens, X.L. Wu, and B. Zhang: Corrosion behavior of AZ21, AZ501 and AZ91 in sodium chloride. *Corros. Sci.* **40,** 1769 (1998).
6. S. Mathieu, C. Rapin, J. Steinmetz, and P. Steinmetz: A corrosion study of the main constituent phases of AZ91 magnesium alloys. *Corros. Sci.* **45,** 2741 (2003).
7. D.L. Albright: Relationship of microstructure and corrosion behavior in magnesium alloy ingots and castings, in *Advances in Magnesium Alloys and Composites,* edited by H.G. Paris and W.H. Hunt, (International Magnesium Association and the Non-Ferrous Metals Committee Symp. Proc, TMS, Warrendale, PA, 1988), p. 57.
8. G. Baril and N. Pébère: The corrosion of pure magnesium in aerated and deaerated sodium sulphate solution. *Corros. Sci.* **43,** 471 (2001).
9. J. Chen, J. Wang, E. Han, J. Dong, and W. Ke: Corrosion behavior of AZ91D magnesium alloy in sodium sulfate solution. *Mater Corros.* **57,** 789 (2006).
10. G. Song, A. Atrens, D. St. John, X. Wu, and J. Naim: The anodic dissolution of magnesium in chloride and sulphate solutions. *Corros. Sci.* **39,** 1981 (1997).
11. G. Baril, G. Galicia, C. Deslouis, N. Pebere, B. Ttibollet, and V. Vivier: An impedance investigation of the mechanism of pure magnesium corrosion in sodium sulfate solutions. *J. Electrochem. Soc.* **154,** 108 (2007).
12. G.L. Song and A. Atrens: Understanding magnesium corrosion—A framework for improved alloy performance. *Adv. Eng. Mater.* **5,** 837 (2003).
13. H. Kuwahara, Y. Al-Abdullat, M. Ohta, S. Tsutsumi, K. Ikeuchi, and N. Mazaki: Surface reaction of magnesium in Hank's solutions. *Mater. Sci. Forum* **350,** 349 (2000).
14. H. Kuwahara, Y. Al-Abdullat, N. Mazaki, S. Tsutsumi, and T. Aizawa: Precipitation of magnesium apatite on pure magnesium surface during immersing in Hank's solution. *Mater. Trans.* **42,** 1317 (2001).
15. H. Kuwahara, N. Mazaki, M. Mabuchi, C. Wein, and T. Aizawa: Behavior of magnesium in Hank's solution aimed to trabecular pattern of natural bone. *Mater. Sci. Forum* **419,** 1007 (2003).
16. F. Witte, V. Kaese, H. Haferkamp, E. Switzer, A. Meyer-Lindenberg, C.J. Wirth, and H. Windhagen: In vivo corrosion of four magnesium alloys and the associated bone response. *Biomaterials* **26,** 3557 (2005).
17. F. Witte, J. Fischer, J. Nellesen, H-A. Crostack, V. Kaese, A. Pisch, F. Beckmann, and H. Windhagen: In vitro and in vivo corrosion measurements of magnesium alloys. *Biomaterials* **27,** 1013 (2006).
18. Y.J. Zhang, C.W. Yan, F.H. Wang, and W.F. Li: Electrochemical behavior of anodized Mg alloy AZ91D in chloride containing aqueous solution. *Corros. Sci.* **47,** 2816 (2005).
19. S.B. Cho, K. Nakanishi, T. Kokubo, N. Soga, C. Ohtsuki, T. Nakamura, T. Kitsugi, and T. Yamamuro: Dependence of apatite formation on silica-gel on its structure—effect of heat-treatment. *J. Am. Ceram. Soc.* **78,** 769 (1995).
20. S.V. Golubev, O.S. Pokrovsky, and V.S. Savenko: Unseeded precipitation of calcium and magnesium phosphates from modified seawater solutions. *J. Cryst. Growth* **205,** 354 (1999).
21. J. Weng, Q. Liu, J.G.C. Wolke, X.D. Zhang, and K. deGroot: Formation and characteristics of the apatite layer on plasma-sprayed hydroxyapatite coatings in simulated body fluid. *Biomaterials* **18,** 1027 (1997).
22. L.T. Canham and C.L. Reeves: Apatite nucleation on low porosity silicon in acellular simulated body fluid, in *Thin Films and Surfaces for Bioactivity and Biomedical Applications,* edited by C.M. Cotell, A.E. Meyer, S.M. Gorbatkin, and G.L. Grobe III (Mater. Res. Soc. Symp. Proc. **414,** Pittsburgh, PA, 1996), p. 189.
23. C.L. Shao, H.Y. Guan, and Y.C. Liu: MgO nanofibres via an electrospinning technique. *J. Mater. Sci.* **41,** 3821 (2006).
24. J.C. Elliot: Structure and chemistry of the apatites and other calcium orthophosphates, in *Studies in Inorganic Chemistry*. Vol. 18 (Elsevier, Amsterdam, 1994), p. 27.
25. M.F. Morks: Magnesium phosphate treatment for steel. *Mater. Lett.* **58,** 3316 (2004).
26. L.C. Li, J.C. Gao, and Y. Wang: Evaluation of cyto-toxicity and corrosion behavior of alkali-heat-treated magnesium in simulated body fluid. *Surf. Coat. Technol.* **185,** 92 (2004).
27. B.A. Shaw: Corrosion resistance of magnesium alloys, in *Corrosion: Fundamentals, Testing and Protection*, ASM Handbook Vol. 13a, edited by S.D. Cramer and B.S. Covino (ASM International, USA, 2003), p. 692.
28. G. Song, A. Atrens, D. St. John, X. Wu, and J. Nairn: The anodic dissolution of magnesium in chloride and sulphate solutions. *Corros. Sci.* **39,** 1981 (1997).
29. G.L. Song and A. Atrens: Corrosion mechanisms of magnesium alloys. *Adv. Eng. Mater.* **1,** 11 (1999).